Nuclear Engineering and Technology 55 (2023) 1400–1409

Contents lists available at ScienceDirect

Nuclear Engineering and Technology

journal homepage: www.elsevier.com/locate/net

Original Article

Assessment of CUPID code used for condensation heat transfer analysis under steam-air mixture conditions

Ji-Hwan Hwang, Jungjin Bang, Dong-Wook Jerng*

School of Energy Systems Engineering, Chung-Ang University, 84 Heukseok-ro, Dongjak-gu, Seoul, 06974, Republic of Korea

ARTICLE INFO

Article history:
Received 5 July 2022
Received in revised form
19 December 2022
Accepted 25 December 2022
Available online 27 December 2022

Keywords:
Condensation heat transfer
Non-condensable gas
Steam diffusion
Computational fluid dynamics
Condensation models

ABSTRACT

In this study, three condensation models of the CUPID code, i.e., the resolved boundary layer approach (RBLA), heat and mass transfer analogy (HMTA) model, and an empirical correlation, were tested and validated against the COPAIN and CAU tests. An improvement on HMTA model was also made to use well-known heat transfer correlations and to take geometrical effect into consideration. The RBLA was a best option for simulating the COPAIN test, having mean relative error (MRE) about 0.072, followed by the modified HMTA model (MRE about 0.18). On the other hand, benchmark against CAU test (under natural convection and occurred on a slender tube) indicated that the modified HMTA model had better accuracy (MRE about 0.149) than the RBLA (MRE about 0.314). The HMTA model with wall function and the empirical correlation underestimated significantly, having MRE about 0.787 and 0.55 respectively. When using the HMTA model, consideration of geometrical effect such as tube curvature was essential; ignoring such effect leads to significant underestimation. The HMTA and the empirical correlation required significantly less computational resources than the RBLA model. Considering that the HMTA model was reasonable accurate, it may be preferable for large-scale simulations of containment.

1. Introduction

Condensation in the presence of noncondensable gases is an important form of heat transfer in refrigerators, heat exchangers, air-conditioners, and distillation. In the field of nuclear engineering, studies on condensation heat transfer have been made as it affects the containment pressure and temperature, when steam is released to the containment and condenses on the wall and structures. Moreover, steam condensation in presence of noncondensable gases draws a lot of attention as it is key phenomenon for passive safety systems which are being developed, such as passive containment cooling system (PCCS) [1]. The PCCS depressurize the containment by condensing vapor, and transferring heat to a heat sink external to the containment. The PCCS being developed in Korea comprised a heat exchanger with multiple tubes, a water tank installed outside the containment and connecting pipes, and the steam condensation occurs outside of the condensing tube.

Various wall condensation models have been proposed for to predict steam condensation in presence of noncondensable gases. The wall condensation models includes the empirical correlation, the heat and mass transfer analogy (HMTA) model and the resolved boundary layer approach (RBLA). In case of the empirical correlation, the Uchida [2] and Tagami [3] are the correlations which have mass fraction of noncondensable gas as only variable, unlike the correlation developed more recently consists pressure, wall subcooling and vapor mass fraction as variable [4–8]. The Uchida and Tagami correlation were adopted in thermal-hydraulic code for containment pressure and temperature analysis, such as CONTEMPT-LT [9,10]. Although the Uchida and Tagami model are thought to provide underestimated condensation heat transfer rate, those were widely used for analysis so that results could be conservative.

In recent days, due to the enhancement of computing capability, attempts to analyze the behavior of atmosphere when condensation occurs in high resolution have been made using the computational fluid dynamics (CFD) code. Using the fine mesh, the boundary layer in vicinity of condensing surface is resolved (RBLA), and the condensation heat transfer is calculated based on the steam diffusion process. The RBLA can provide detailed thermal-hydraulic behavior near condensing surface and in complex geometry. Bucci et al. [11] compared a heat and mass transfer diffusion method (HMTDM), and compared with its results with that predicted with a

* Corresponding author.
E-mail address: dwjerng@cau.ac.kr (D.-W. Jerng).

https://doi.org/10.1016/j.net.2022.12.032

model based on heat and mass transfer analogy (HMTA). Ambrosini et al. [12–15] performed CFD simulations under a pure steam condition, under a noncondensable gas present condition, and under a high-buoyancy condition and compared the result with that predicted with other model such as HMTA and empirical correlation. Dehbi et al. [16] benchmarked the wall condensation model of the ANSYS CFD code against the COPAIN [17], Uchida [2], Tagami [3], Dehbi [4] and TOSQAN [18,19] experiment, and concluded that CFD simulation would provide reasonable estimation on condensation heat transfer. Vyskocil et al. [20] validated a condensation model based on FLUENT code against the CONAN [13] and PANDA [21] tests. Jeon et al. [22] performed CFD simulations to explore the effects of geometrical parameters (tube inclination and curvature).

If the PCCS mission time is taken to be 72 h (a generally accepted value [23]), estimation of PCCS performance and simulation of the containment atmospheric conditions using the CFD code is very difficult as it requires massive computational resources. The HMTA model can be used instead, to reduce the computational resource requirement. The HMTA calculates condensation rate from the mass transfer coefficient, which can be obtained by applying heat and mass transfer analogy to the heat transfer coefficient. For heat transfer coefficient calculation, well-known correlation such as McAdams correlation [24] are often used [25,26], and the wall function [27] which generally used in commercial CFD codes are also used [28]. The HMTA was adopted not only for lumped parameter code like MARS-KS [29], MELCOR [30], GOTHIC [31] but also used in CFD code like GASFLOW [32]. The usage of HMTA model can reduces the required computing resources even in CFD code, as the model requires coarse mesh to use the bulk material properties. However, as the coarse mesh ignores the geometrical effect, such as curvature effect which is known to have considerable enhancement in condensation heat transfer [33–35].

Thus, selection of an appropriate condensation model is essential when performing large-scale simulations, particularly including PCCS which have complex and curved surfaces. However, not many researches compared the condensation models with same code, particularly for the condition under natural convection on a curved surface.

Therefore, we compared condensation models of the CUPID, a CFD code developed by the Korean Atomic Energy Research Institute (KAERI). The models tested in this paper includes the RBLA model, the HMTA model, and an empirical correlation. Condensation models were tested in steam-air mixtures under both forced and natural convection regimes, and in vertical flat plate and vertical tube geometry. The rest of the paper is organized as follows: the details of chosen experiments are described in Section 2, Section 3 presents the description of condensation models, Section 4 presents benchmarking results and Section 5 provides the study conclusions.

2. Description on condensation heat transfer experiments

2.1. The COPAIN test

The COPAIN test was conducted to identify condensation heat transfers in the presence of noncondensable gases [17]. The experiment was conducted under forced convection conditions; the steam-air mixture was injected into the top of the vertical channel. In the conditions we considered, the injection velocity varied from 0.3 to 3 m/s. The rectangular vertical channel was 2.5 m in height, 0.6 m in width, and 0.5 m in depth. Condensation occurred on a vertical plate 2.0 m in height and 0.6 m in width. A schematic of the test facility is shown in Fig. 1 and the test conditions are listed in Table 1.

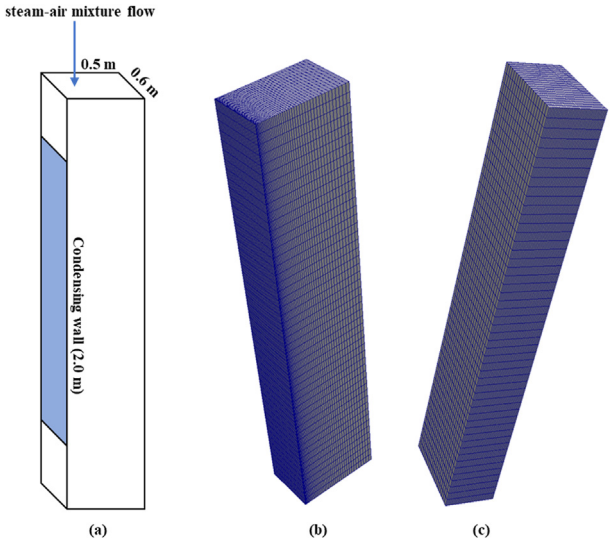

Fig. 1. (a) Schematic of the COPAIN test facility; (b) computational grid for the RBLA and (c) HMTA and Uchida models.

2.2. Description of the CAU test

Condensation heat transfer in a steam-air mixture under a natural convection regime was experimentally analyzed at the experimental facility of Chung-Ang University, which has a 2.0-m high pressure vessel (0.447 m in diameter). Condensation occurred on a 0.75-m high tube (0.0381 m in diameter). The condensing tube was installed at the center of the pressure vessel. The temperature of the coolant was controlled using a preheater and a chiller, and the mass flow rate was controlled using a pump. The coolant flowed from the bottom to the top. The vessel was filled with air, and steam was injected at the bottom to ensure mixing of the steam and air. A schematic of the test is shown in Fig. 2.

As steam was supplied from the bottom of the pressure vessel, and due to the occurrence of the condensation and cooling, a vigorous natural circulation inside the pressure vessel was occured. The test conditions are listed in Table 2. Unlike the COPAIN test (which measures condensation heat flux along a vertical plate [17]), the CAU test measures condensation heat transfer coefficients, which were obtained by dividing heat flux by wall subcooling.

$$\overline{h} = \frac{q''_{tot}}{\overline{T}_\infty - \overline{T}_w} = \frac{\dot{m}_{coolant} C_p \left(T_{coolant,out} - T_{coolant,in}\right)}{\overline{T}_\infty - \overline{T}_w} \tag{1}$$

3. Model description

3.1. The CUPID model description

The CUPID code is a three-dimensional, thermal-hydraulic analysis code developed at KAERI. CUPID uses two-fluid (liquid and gas) and three-field (liquid, liquid droplets, and gas) conservation equations. Other equations deal with noncondensable gas conservation; there are also equations of state. The continuity equation of CUPID is:

$$\frac{\partial}{\partial t}\left(\alpha_g \rho_g\right) + \nabla \cdot \left(\alpha_g \rho_g \vec{u}_g\right) = \dot{S}_g + \Gamma_w \tag{2}$$

The energy conservation equation is:

Table 1
COPAIN test conditions.

	Velocity (m/s)	Pressure (bar)	Bulk temperature (K)	Wall temperature (K)	NC gas mass fraction
P0441	3	1.02	353.23	307.4	0.767
P0443	1	1.02	352.33	300.06	0.772
P0344	0.3	1.02	351.53	299.7	0.773

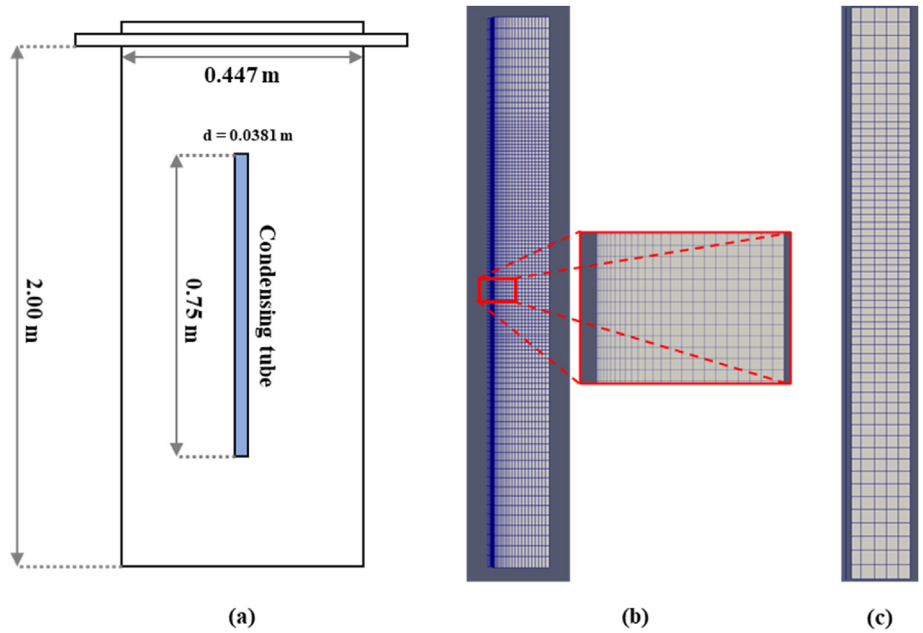

Fig. 2. (a) Schematic of the CAU test facility; (b) the computational grids for RBLA and (c) the HMTA and Uchida models.

$$\frac{\partial}{\partial t}\left(\alpha_g \rho_g e_g\right) + \nabla \cdot \left(\alpha_g \rho_g e_g \vec{u}_g\right) = \dot{S}_g + \Gamma_w h_{fg} \tag{3}$$

where Γ represent the volumetric condensation rate. Steam condensation in the presence of noncondensable gases is greatly affected by steam diffusion; we dealt with this using the method of Wilke and Lee [36]:

$$D = \frac{10^{-3} T^{1.5}\left[3.03 - \left(\frac{0.98}{M_{AB}^{0.5}}\right)\right]}{P M_{AB}^{0.5} \sigma_{AB}^2 \Omega_D} \tag{4}$$

where $M_{AB}^{0.5}$ is $2(1/M_A + 1/M_B)^{-1}$. In Eq. (4), M, σ, and Ω represent the molecular weight, Lennard-Jones collision diameter, and dimensionless collision integral, respectively. The value of σ is taken from Wilke and Lee [36] and the value of Ω can be obtained using the method of Poling [37]. The CUPID code incorporates several turbulent models, including the SST K-w, standard K-e, realizable K-e and RNG K-e models. The CUPID code also incorporates low-Reynolds K-e and turbulent buoyancy models. In this paper, the K-e model was used.

The timestep of CUPID simulation is automatically controlled based on the Courant number ($u\Delta t/\Delta x$). If the Courant number calculated in the computation domain exceeds a user-defined maximum, the timestep is halved until the Courant number becomes less than 1. The simulation was continued until the condensation heat flux and condensation heat transfer coefficient reached steady states.

3.2. Description of wall condensation models

As default, the CUPID code incorporates three wall condensation models: the RBLA, the HMTA model, and the empirical correlation of Uchida [2].

3.2.1. Resolved boundary layer approach

The RBLA is a mechanistic model that calculates the condensation rate based on steam diffusion in multicomponent mixtures. The equation for the RBLA is as follows:

$$\Gamma_w = -\frac{1}{Y_s - 1}\rho_g D \frac{\partial Y_s}{\partial n}\frac{A_w}{V_{cell}} \tag{5}$$

where Γ, Y, ρ, and D represent the volumetric condensation rate, mass fraction, density, and diffusion coefficient, respectively. The subscripts s and g refer to steam and gas, respectively. A_{wall} and V_{cell} are the area of the wall and volume of the cell next to the wall, respectively. In vigorous condensation conditions, a suction effect take place at phase change interface, and the steam supplement to the condensing wall would be enhanced. Therefore, a correction factor for suction effect should be adopted for the RBLA model [16,38]. In this paper, a most commonly used suction factor proposed by Bird et al. [39] was adopted:

$$\Gamma_{RBLA} = -\frac{1}{Y_s - 1}\rho_g D \frac{\partial Y_s}{\partial n}\frac{A_{wall}}{V_{cell}}\frac{\ln(1+B)}{B} \tag{6}$$

Bird suction parameter B can be calculated as $(Y_{s,w} - Y_{s,\infty})/(1 - Y_{s,w})$.

Table 2
The CAU test conditions.

	Pressure (bar)	Bulk temperature (K)	Wall temperature (K)	NC gas mass fraction
Case #1	1.99	387.24	358.39	0.252
Case #2	2.04	375.33	343.24	0.577
Case #3	2.01	363.64	338.40	0.746
Case #4	3.96	408.12	379.57	0.300
Case #5	3.96	396.00	365.01	0.570
Case #6	3.97	382.84	353.01	0.743

3.2.2. Heat and mass transfer analogy model with wall function

The equation for the HMTA model implemented in CUPID is as follows:

$$\Gamma_w = -h_m \rho_g \ln\left(\frac{1-Y_{s,w}}{1-Y_{s,\infty}}\right) \tag{7}$$

where the mass transfer coefficient, h_m, is calculated as follows:

$$h_m = h_{conv}\left(\frac{D}{k_g}\right)\left(\frac{Sc}{Pr}\right)^{1/3}. \tag{8}$$

In Eq. (8), h_{conv}, k, Sc, and Pr represent the heat transfer coefficient, thermal conductivity, Schmidt number, and Prandtl number, respectively. Originally, the CUPID code uses a standard wall function to obtain the heat transfer coefficient [27]:

$$h_{conv} = \frac{(T_w - T_g)\rho c_p u^*}{(T_w - T_\infty)Pr_t\left[\frac{1}{\kappa}\ln(Ey^*) + P\right]} \tag{9}$$

where P can be calculated by the formula proposed by Jayatilleke [40]. In Eq. (9), T_g, u^*, κ, E, Pr_t and y^* represent the gas temperature at the cell next to the condensing surface, friction velocity, von Karman constant (0.4187), an empirical constant (9.793), turbulent Prandtl number (0.9) and the dimensionless wall distance, respectively. Therefore, the HMTA model with wall function can be expressed as:

$$\Gamma_{HMTA,wf} = -\frac{(T_w - T_g)\rho c_p u^*}{(T_w - T_\infty)Pr_t\left[\frac{1}{\kappa}\ln(Ey^*) + P\right]} \times \left(\frac{D}{k_g}\right)\left(\frac{Sc}{Pr}\right)^{1/3} \rho_g \ln\left(\frac{1-Y_{s,w}}{1-Y_{s,\infty}}\right) \tag{10}$$

The dimensionless wall distance (Y^+) should exceed 30 when using the HMTA model with wall function.

3.2.3. Empirical correlation

Finally, CUPID incorporates the empirical correlation proposed by Uchida [2]:

$$h_{uchida} = 380\left(\frac{Y_{s,\infty}}{1-Y_{s,\infty}}\right)^{0.707} \tag{11}$$

As the Uchida model is presented as forms of the heat transfer coefficient, CUPID calculates the volumetric condensation rate as follows:

$$\Gamma_{Uchida} = -\frac{h_{uchida}(T_{sat} - T_{wall})}{h_{fg}} \tag{12}$$

where T and h_{fg} represent the temperature and heat of vaporization, respectively. Although the CUPID code supports the consideration of condensate film, the condensate film was not considered in this study, as the thermal resistance of condensate film is ignorable due to thin condensate film.

3.3. Modification on the heat and mass transfer analogy model with heat transfer correlations

Although the model with the standard wall function is reasonably accurate for forced convection regime [41], usage of wall function may yield underestimation in natural convection regime [42] as the standard wall function had worked out for forced convection regime. Therefore, accuracy can be enhanced by considering models appropriate for the convection regime. Under forced convection conditions, the local heat transfer coefficient can be calculated as [43]:

$$h_g = 0.0296 \mathrm{Re}_x^{4/5}\ \mathrm{Pr}^{1/3}\frac{k}{x} \tag{13}$$

In natural convection conditions, the heat transfer coefficient can be calculated as [24]:

$$h_g = 0.13(Gr_x\ \mathrm{Pr})^{1/3}\frac{k}{x} \tag{14}$$

Therefore, the modified HMTA model under forced convection conditions is given by:

$$\Gamma_{HMTA,FC} = -0.0296 \mathrm{Re}_x^{4/5}\ \mathrm{Pr}^{1/3}\frac{k}{x}\rho_g \ln\left(\frac{1-Y_{s,w}}{1-Y_{s,\infty}}\right)\left(\frac{D}{k_g}\right)\left(\frac{Sc}{Pr}\right)^{1/3} \tag{15}$$

Under natural convection conditions, the modified HMTA model is given by:

$$\Gamma_{HMTA,NC} = -0.13(Gr_x\ \mathrm{Pr})^{1/3}\frac{k}{x}\rho_g \ln\left(\frac{1-Y_{s,w}}{1-Y_{s,\infty}}\right)\left(\frac{D}{k_g}\right)\left(\frac{Sc}{Pr}\right)^{1/3} \tag{16}$$

Note that the suction factor is already implemented in the HMTA model.

When the HMTA model is used, a coarse mesh should be used as the correlation used to obtain the mass transfer coefficient requires material properties evaluated at bulk condition. However, this may lead to inconsideration of the geometrical effect such as curvature effect which occurs on a condensing tube. Moreover, as the correlation which chose to estimate the mass transfer coefficient were developed in different geometry with that considered in this paper, a correction would be needed. Therefore, the curvature effect (in the case of benchmarking the CAU test) and the entrance effect (in the case of benchmarking the COPAIN test), were applied to the model.

On a curved surface, the velocity and temperature gradients change, and the heat transfer thus also changes [44]; this is known as the curvature effect. Note that most CFD codes calculate the velocity and temperature gradients in the boundary layer, and thus automatically consider curvature effect. As the CAU tests were

conducted under turbulent free convection condition, the curvature effect factor as follows was used [35]:

$$\theta = \frac{Nu}{Nu_{FP}} = 1 + 1.23\left(\frac{2g\beta\Delta T}{\mu^2 d}\right)^{0.357} \quad (17)$$

For the conditions which steam-air mixture was injected at the top of the channel such as the COPAIN test, the change of condensation heat transfer in the entrance region should be adopted [42,45]. The entrance effect factor proposed by Reynolds et al. [46] was used:

$$Nu = Nu_0\left(1 + \frac{0.8\left(1 + 70000\mathrm{Re}^{-3/2}\right)}{x/d}\right). \quad (18)$$

The entrance effect factor was applied to the HMTA model when simulating the COPAIN test. Note that the RBLA and Uchida model was not affected, as the former calculates the change of concentration gradient mechanistically and the latter is an empirical correlation.

4. Comparision of the condensation models

4.1. Computation grid used for the COPAIN test

As mentioned above, the mechanistic model using the RBLA, which solves the vapor concentration gradient near the wall, requires a fine mesh. On the other hand, the HMTA and Uchida models use bulk and wall properties; the models thus require a coarse mesh ($Y^+ > 30$). Therefore, different computation grids were used depending on the model. The wall Y^+ values of the computation grids used in the COPAIN test benchmarking are listed in Table 3. The condensation heat flux along vertical wall in various Y^+ are shown in Fig. 3. It could be found that when using RBLA, the condensation heat flux did not change with Y^+ if it was less than about 6. Therefore, using the computation grid which have Y^+ about 5 when using RBLA would provide reasonable result. The condensation heat flux along vertical wall calculated with modified HMTA model in various Y^+ yielded similar results, indicating that the usage of computation grid which have Y^+ about 30–40 would provide reasonable results.

4.2. Results of COPAIN test benchmarking

Fig. 4 shows the benchmarking results. The mean relative error (MRE) and standard deviation (SD) was calculated to statistically analyze the deviations between predicted and experimental value. The mean relative error was calculated as follows:

$$MRE = \frac{1}{n}\sum_i^n \frac{\Gamma_{CUPID,i} - \Gamma_{\mathrm{exp},i}}{\Gamma_{\mathrm{exp},i}} \quad (19)$$

The standard deviation was calculated as follows:

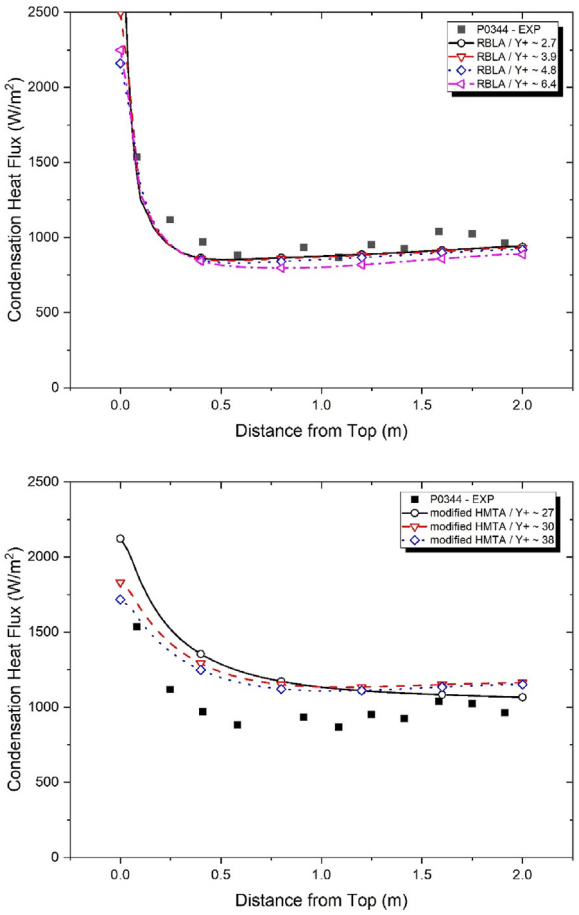

Fig. 3. Condensation heat flux along vertical wall; (top) using RBLA with various Y^+ mesh (bottom) using HMTA with various Y^+ mesh.

$$SD = \sqrt{\frac{\sum_i^n \left(\frac{\Gamma_{CUPID,i} - \Gamma_{\mathrm{exp},i}}{\Gamma_{\mathrm{exp},i}}\right)^2}{n-1}} \quad (20)$$

In Eqs. (19)-(20), n represents amount of data. The evaluation of MRE and SD was conducted in 11 elevations, and the average of each case is shown in Table 4. The statistical analysis showed that the usage of RBLA model gives a best prediction on the condensation heat transfer, followed by the modified HMTA model. The HMTA model with wall function showed less accuracy than the modified HMTA model, yet provided better result than the Uchida model.

In Fig. 4, The RBLA estimated the condensation heat flux along the vertical plate most accurately. In particular, the RBLA predicted the change in condensation heat flux at high elevations, attributable to the fact that the RBLA calculates velocity and temperature gradient in the boundary layer using the fine mesh.

The modified HMTA model (Eqs. (15)-(16)) yielded reasonable

Table 3
Computation grids used for COPAIN test benchmarking.

	Y^+ (RBLA)	Y^+ (HMTA & Uchida)	Thickness of near-wall cell (RBLA)	Thickness of near-wall cell (HMTA & Uchida)	Total cell count (RBLA)	Total cell count (HMTA & Uchida)
P0441	5.37	29.06	0.0007	0.00339	165,600	31,200
P0443	4.65	37.87	0.0013	0.01018	141,600	25,700
P0344	4.88	38.14	0.0020	0.02541	117,200	15,600

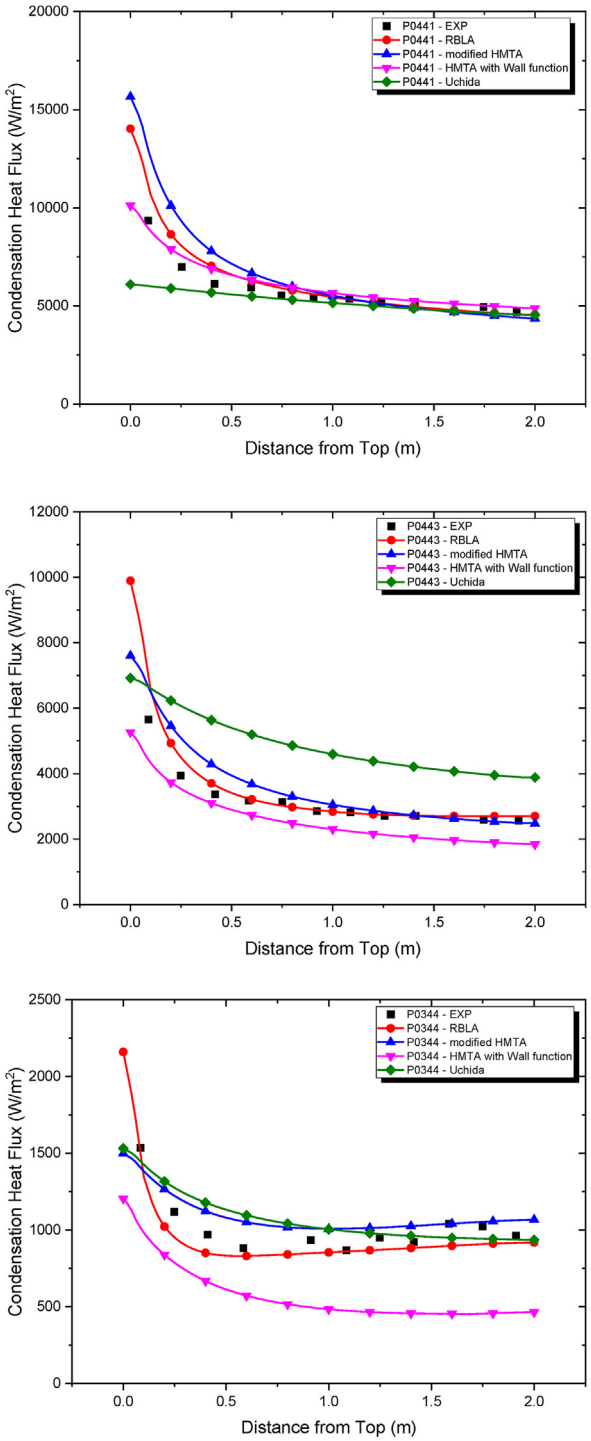

Fig. 4. Results of the COPAIN test benchmarking (top) P0441 case, (middle) P0443 case, (bottom) P0334 case.

results and predicted heat flux change along the height. The adoption of entrance effect factor provided capability to estimate the condensation heat flux change along the vertical plate. However, overestimation was found at high elevations. This was attributable to the limitation of adopted entrance effect factor as it should only be used for the range of $3000 < Re < 50{,}000$ and the Reynolds number at the region near steam-air inlet would be lower than 3000. The HMTA model with wall function, also provided reasonable accuracy. The HMTA model with wall function provided higher accuracy than the modified HMTA model in high velocity condition (P0441), but considerably underestimated in the case of low velocity condition (P0344). Therefore, the HMTA model with wall function would be appropriate for forced convection conditions with high velocity, yet the modified HMTA model can be used for various atmosphere velocity conditions particularly for low velocity conditions.

Finally, the Uchida model exhibited large deviations as the test conditions varied. The discrepancies in condensation heat flux predictions are attributable to the inconsideration of thermal-hydraulic conditions such as velocity, bulk pressure and wall subcooling in the correlation.

4.3. Computation grid used for the CAU test

As done in COPAIN test benchmarking, the computational grids were also adjusted to meet the requirements of the condensation models when benchmarking the CAU test. The wall Y^+ values of the grids used for CAU test benchmarking are listed in Table 5.

4.4. Results of CAU test benchmarking

The statistical analyses results are shown in Table 6. In average, the MRE and SD of the modified HMTA model provided best prediction, followed by the RBLA model. The prediction result of the HMTA model with wall function and Uchida model showed a significant deviation with experimental data.

The benchmarking results are shown in Fig. 5. Unlike in the COPAIN test benchmarking, the CAU test benchmarking indicated that the RBLA model and Uchida model underestimated the heat transfer coefficient. The underestimation of Uchida model is probably attributable to the lack of consideration of the thermal-hydraulic conditions (as stated in Section 4.2). The underestimation of RBLA model is probably attributed to the inconsideration of diffusion-driven flow in condensation model and convective heat transfer. Due to vigorous steam diffusion, the diffusing steam drags the gas mixture towards the condensing surface, increasing the steam supplement hence enhancing the condensation rate. The modified HMTA model (Eqs. (15)-(16)) predicted the experimental heat transfer coefficients reasonably accurately, providing the best accuracy among the condensation models tested in this study while the HMTA model with wall function provided least accuracy among the models. The underestimation of the HMTA model with wall function is attributable to the usage of standard wall function, which was developed based on the forced convection regime [42].

Table 4
Statistical analysis of COPAIN test benchmarking result.

	MRE				Standard Deviation			
	RBLA	Modified HMTA	HMTA/WF	UCHIDA	RBLA	Modified HMTA	HMTA/WF	UCHIDA
P0441	0.074	0.136	0.053	0.091	0.010	0.035	0.004	0.017
P0443	0.065	0.113	0.190	0.549	0.011	0.022	0.039	0.317
P0344	0.078	0.286	0.442	0.105	0.008	0.087	0.205	0.016
Average	0.072	0.179	0.228	0.248	0.010	0.048	0.083	0.117

Table 5
Computation grids used for CAU test benchmarking.

	Y^+ (RBLA)	Y^+ (HMTA & Uchida)	Thickness of near-wall cell (RBLA)	Thickness of near-wall cell (HMTA & Uchida)	Total cell count (RBLA)	Total cell count (HMTA & Uchida)
Case #1	4.77	22.79	0.001	0.1143	110,000	580
Case #2	5.03	25.06	0.001	0.1143	110,000	580
Case #3	4.25	22.63	0.001	0.1143	110,000	580
Case #4	3.54	26.78	0.0005	0.1143	171,600	580
Case #5	2.02	30.97	0.0005	0.1143	171,600	580
Case #6	2.95	32.18	0.0005	0.1143	171,600	580

Table 6
Statistical analysis of CAU test benchmarking result.

	MRE				Standard Deviation			
	RBLA	Modified HMTA	HMTA/WF	UCHIDA	RBLA	Modified HMTA	HMTA/WF	UCHIDA
P = 2 bar	0.255	0.169	0.753	0.589	0.278	0.226	0.753	0.629
P = 4 bar	0.373	0.129	0.821	0.511	0.377	0.137	0.821	0.512
Average	0.314	0.149	0.787	0.550	0.327	0.182	0.787	0.570

Therefore, it is apparent that selecting a correlation that fits the flow regime is essential when using the HMTA model.

4.5. Effect of correction factors

As the heat flux at high elevation is about 50% to more than 100% higher than that in low elevation, enhancing the heat flux prediction in high elevation is critical. Fig. 6 shows the enhancement of heat flux prediction due to adopting entrance effect, in P0443 and P0344 case of the COPAIN test. At the top of the condensing surface, the noncondensable gas boundary layer is thinner than that located at the bottom. Due to thin noncondensable gas boundary layer, the heat and mass transfer resistance is significantly weaker; the steam is supplied to the condensing surface more actively. Therefore, the condensation heat flux becomes higher than the other elevation. Although the adoption of the entrance effect causes little over-prediction at lower elevation, it made it possible to calculate the high heat flux at high elevation.

The curvature effect factor which was used for benchmarking against the CAU test showed significant effect. At the curved surface, the gas mixture had higher chance to transfer heat and mass with the adjacent gas mixture. Higher heat and mass transfer leads to thinner gas boundary layer and higher steam supplement rate. Therefore, the condensation heat transfer is increased. Fig. 7 shows the change of heat transfer coefficient predicted according to the usage of the curvature effect factor. When the curvature effect was not considered, the modified HMTA model underpredicted heat transfer coefficient about 40–60%, depending on the condition. Therefore, when using the HMTA-based model, the geometrical effect such as tube curvature should be considered.

4.6. Computational requirements

As the RBLA model uses a fine mesh, while the other models use coarse meshes, the grid numbers, and thus also the required computational resources, differ significantly. The time taken for the simulation are shown in Table 7. The simulation was conducted on a system using i9-12900K with a single core.

The RBLA required significantly more resources than the HMTA

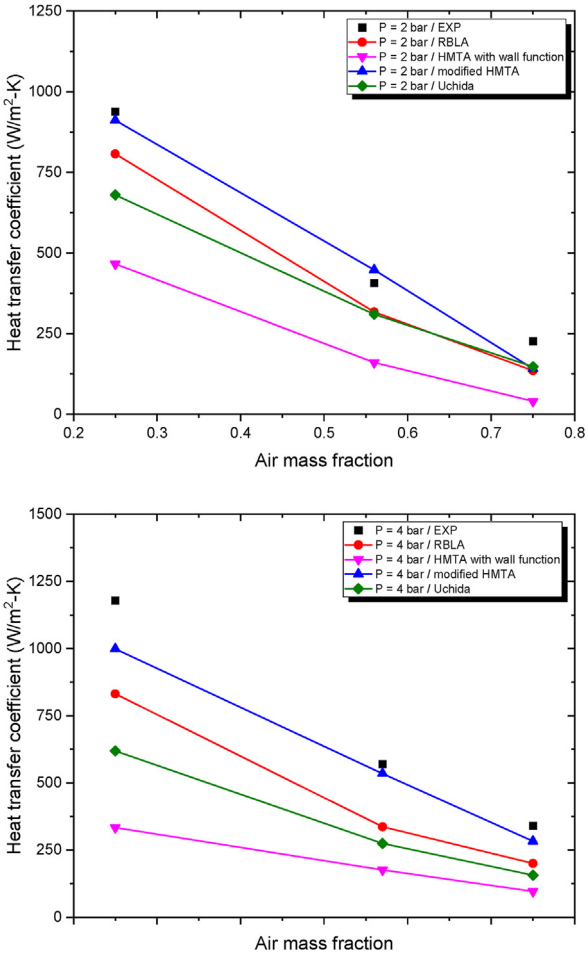

Fig. 5. Results of the CAU tests benchmarking (top) pressure = 2 bar condition, (bottom) pressure = 4 bar condition.

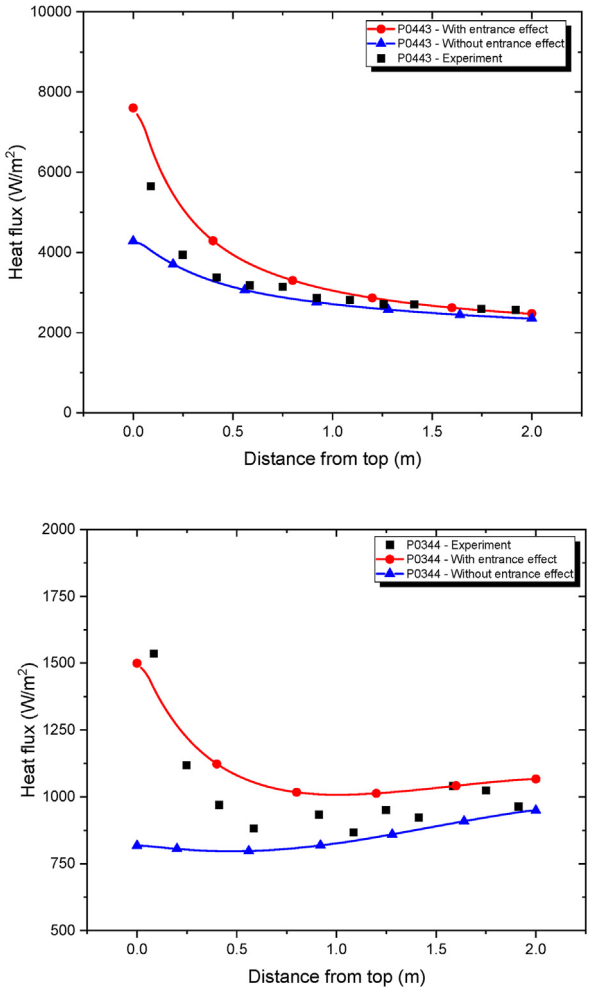

Fig. 6. Effect of entrance effect factor adoption, (top) COPAIN-P0443 case, (bottom) COPAIN-P0344 case.

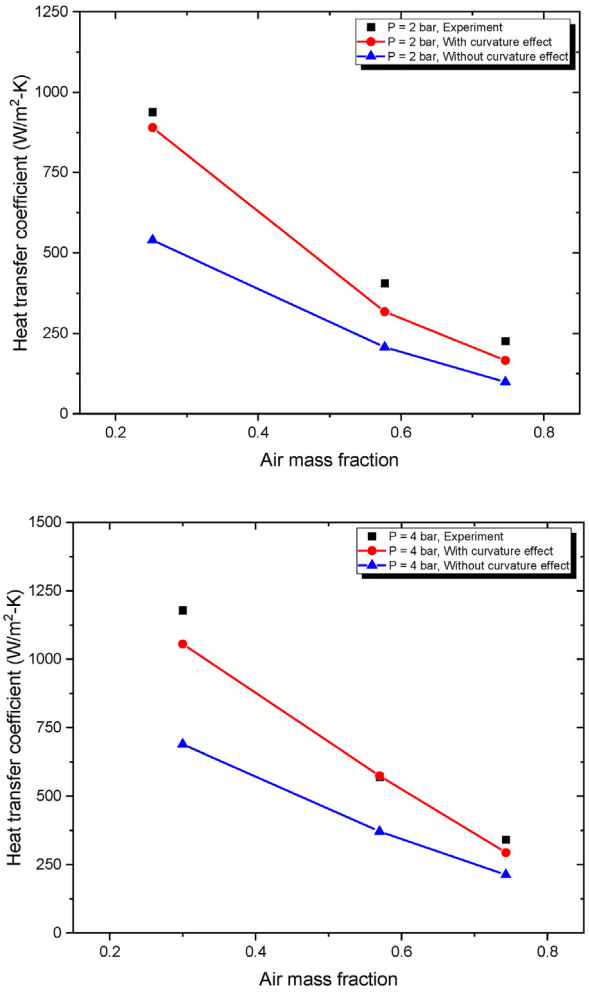

Fig. 7. Effect of curvature effect factor adoption, (top) CAU-2 bar condition, (bottom) CAU-4 bar condition.

and Uchida models. Given the simulation results presented in Section 4.2 and 4.4, it can be concluded that the HMTA model has reasonable accuracy and minimal computation requirements.

5. Conclusions

The condensation models of the CUPID code were assessed by benchmarking against the COPAIN and CAU tests, reflecting condensation under forced and natural convection regimes, respectively. Four models, a RBLA, two HMTA-based models, and empirical correlation (Uchida) were tested, and the results were compared. In addition to the HMTA model which uses Spalding wall function, a modified HMTA model which uses well-known heat transfer correlation such as McAdams were proposed. In the case of the modified HMTA model, geometrical effect factors such as entrance and tube curvature were also adopted.

The RBLA provided best result when benchmarked against the COPAIN test, having about 7.2% error in average. Two HMTA-based model predicted heat flux with about 18% (modified one) and 23% error (HMTA model with wall function) in average. The Uchida model, which had widely used for containment pressure/temperature analysis, had highest error among the models. In particular, the RBLA and the modified HMTA models also predicted heat flux changes at higher elevations with reasonable accuracy, even at low velocities; the Uchida model was less satisfactory in this respect. However, in the benchmark against the CAU test, which was under a natural convection regime, the results were different; the modified HMTA model was most accurate among four models, having about 15% error in average. The other models underestimated the condensation heat transfer; the RBLA predicted heat transfer coefficient with about 31.4% error, the HMTA with wall function had about 78.7% error, and the Uchida model had about 55% error. Therefore, those models may require additional modifications for practical application.

A comparison conducted with the modified HMTA model showed the importance of taking geometrical effects such as entrance effect and curvature effect into consideration when using the HMTA-based model. The usage of coarse mesh correlation and made the model vulnerable on condensation heat transfer prediction in different geometry than the correlation originally developed.

Considering the average errors and the computational resource requirements, the modified HMTA model would be the best option for large-scale thermal-hydraulic analyses of containment atmospheres.

Table 7
Computation times required to evaluate 10 physical seconds.

	COPAIN P0441	COPAIN P0344	CAU Case #3	CAU Case #4
RBLA	60125.06	6747.28	10,434.32	57,221.44
HMTA	3826.17	93.50	20.45	21.16
Uchida	3603.23	87.33	19.15	18.57

Declaration of competing interest

The authors declare that they have no known competing financial interests or personal relationships that could have appeared to influence the work reported in this paper.

Acknowledgments

This research was supported by a National Research Foundation of Korea (NRF) grant funded by the Korean government (MSIP: Ministry of Science, ICT and Future Planning) (No. NRF-2017M2B2B1072552)

Nomenclature

A	Area
C_p	Heat capacity at constant pressure
D	Diffusion coefficient
d	Diameter
e	Internal energy
g	Gravitational acceleration
$\overline{h}$	Average heat transfer coefficient
h_{conv}	Convective heat transfer coefficient
h_m	Mass transfer coefficient
h_{fg}	Enthalpy of vaporization
k	Thermal conductivity
M	Molar mass
n	Number of data
Nu	Nusselt number
Pr	Prandtl number
Pr_t	Turbulent Prandtl number
q''	Heat flux
Re	Reynolds number
$\dot{S}$	Source term
Sc	Schmidt number
$\overline{T}$	Average temperature
T	Temperature
$\overrightarrow{u}$	Velocity
u_*	Friction velocity
V	Volume
x	Axial direction
Y	Mass fraction
y*	Dimensionless wall distance
α	Void fraction
β	Thermal expansion coefficient
Γ	Condensation rate
κ	von Karman constant
μ	Dynamic viscosity
ρ	Density
σ	Lennard-Jones collision diameter
Ω	Dimensionless collision integral

Superscript and subscript

cell	Cell
coolant	Coolant
exp	Experiment
in	Inlet
g	gas
out	Outlet
s	Steam
tot	Total
w	Wall
wf	Wall function
∞	Bulk condition

References

[1] C. Byun, D. Jerng, N. Todreas, M. Driscoll, Conceptual design and analysis of a semi-passive containment cooling system for a large concrete containment, Nucl. Eng. Des. 199 (3) (2000) 227–242.
[2] H. Uchida, A. Oyama, Y. Togo, Evaluation of Post-incident Cooling Systems of Light Water Power Reactors, Tokyo Univ., 1965.
[3] T. Tagami, Interim Report on Safety Assessments and Facilities Establishment Project for June 1965, No. 1, Japanese Atomic Energy Research Agency, 1965.
[4] A.A. Dehbi, The Effects of Noncondensable Gases on Steam Condensation under Turbulent Natural Convection Conditions, Massachusetts Institute of Technology, 1991.
[5] H. Liu, N. Todreas, M. Driscoll, An experimental investigation of a passive cooling unit for nuclear plant containment, Nucl. Eng. Des. 199 (3) (2000) 243–255.
[6] M. Kawakubo, M. Aritomi, H. Kikura, T. Komeno, An experimental study on the cooling characteristics of passive containment cooling systems, J. Nucl. Sci. Technol. 46 (4) (2009) 339–345.
[7] J. Su, Z. Sun, G. Fan, M. Ding, Experimental study of the effect of non-condensable gases on steam condensation over a vertical tube external surface, Nucl. Eng. Des. 262 (2013) 201–208.
[8] J. Su, Z. Sun, M. Ding, G. Fan, Analysis of experiments for the effect of noncondensable gases on steam condensation over a vertical tube external surface under low wall subcooling, Nucl. Eng. Des. 278 (2014) 644–650.
[9] Y. Hsii, CONTEMPT: Computer Program for Predicting Containment Pressure-Temperature Response to a Loss-Of-Coolant Accident, Babcock and Wilcox Co., Lynchburg, VA (USA), 1978. Nuclear Power Generation Div.
[10] Y.J. Choo, S.J. Honga, S.H. Hwanga, M.K. Kima, B.C. Leea, S.J. Hab, H. Choib, Performance comparison of containment PT analysis between CAP and CONTEMPT code, in: Transactions of the Korean Nuclear Society Autumn Meeting, 2013. Gyeongju, Korea.
[11] M. Bucci, M. Sharabi, W. Ambrosini, N. Forgione, F. Oriolo, S. He, Prediction of transpiration effects on heat and mass transfer by different turbulence models, Nucl. Eng. Des. 238 (4) (2008) 958–974.
[12] W. Ambrosini, N. Forgione, F. Merli, F. Oriolo, S. Paci, I. Kljenak, P. Kostka, L. Vyskocil, J. Travis, J. Lehmkuhl, Lesson learned from the SARNET wall condensation benchmarks, Ann. Nucl. Energy 74 (2014) 153–164.
[13] W. Ambrosini, N. Forgione, S. Durand, Analysis of experimental data of condensation in the presence of non-condensable gases by a CFD code, in: The International Topical Meeting on Nuclear Reactor Thermal-Hydraulics-NURETH-15, ITA, 2013, pp. 1–12.
[14] W. Ambrosini, M. Bucci, N. Forgione, F. Oriolo, S. Paci, J. Magnaud, E. Studer, E. Reinecke, S. Kelm, W. Jahn, Comparison and analysis of the condensation benchmark results, in: 3rd European Review Meeting on Severe Accident Research (ERMSAR-2008), Citeseer, Nesseber, Bulgaria, 2008.
[15] W. Ambrosini, M. Bucci, N. Forgione, F. Oriolo, S. Paci, Quick look report on SARNET2 condensation benchmark-2 results, Rep. DIMNP RL (2010) 1252.
[16] A. Dehbi, F. Janasz, B. Bell, Prediction of steam condensation in the presence of noncondensable gases using a CFD-based approach, Nucl. Eng. Des. 258 (2013) 199–210.
[17] X. Cheng, P. Bazin, P. Cornet, D. Hittner, J. Jackson, J.L. Jimenez, A. Naviglio, F. Oriolo, H. Petzold, Experimental data base for containment thermal-hydraulic analysis, Nucl. Eng. Des. 204 (1–3) (2001) 267–284.
[18] J. Malet, E. Porcheron, F. Dumay, J. Vendel, Code-experiment comparison on wall condensation tests in the presence of non-condensable gases—numerical calculations for containment studies, Nucl. Eng. Des. 253 (2012) 98–113.
[19] J. Malet, E. Porcheron, J. Vendel, OECD international standard problem ISP-47 on containment thermal-hydraulics—conclusions of the TOSQAN part, Nucl. Eng. Des. 240 (10) (2010) 3209–3220.
[20] L. Vyskocil, J. Schmid, J. Macek, CFD simulation of air–steam flow with condensation, Nucl. Eng. Des. 279 (2014) 147–157.
[21] OECD/SETH-2 Project—PANDA and MISTRA Experiments Final Summary Report (Investigation of Key Issues for the Simulation of Thermal-Hydraulic Conditions in Water Reactor Containment), Nuclear Energy Agency, 2012.
[22] B.G. Jeon, D.Y. Kim, C.W. Shin, H.C. No, Parametric experiments and CFD analysis on condensation heat transfer performance of externally condensing tubes, Nucl. Eng. Des. 293 (2015) 447–457.
[23] J. Bang, J.-H. Hwang, H.G. Kim, D.-W. Jerng, Parametric Analyses for the Design of a Closed-Loop Passive Containment Cooling System, Nuclear Engineering and Technology, 2020.
[24] W.H. Mcadams, Heat Transmission, 3d Ed, McGraw-Hill, 1954.

[25] M. Bucci, Experimental and Computational Analysis of Condensation Phenomena for the Thermal-Hydraulic Analysis of LWRs Containments, University of Pisa, 2009. Ph. D. thesis.
[26] A. Dehbi, A generalized correlation for steam condensation rates in the presence of air under turbulent free convection, Int. J. Heat Mass Tran. 86 (2015) 1–15.
[27] B. Launder, D. Spalding, The numerical computation of turbulent flows, Comput. Methods Appl. Mech. Eng. 3 (2) (1974) 269–289.
[28] D. Wang, L. Tong, X. Cao, Numerical study on the influence of steam condensation on hydrogen distribution in local compartments, Ann. Nucl. Energy 121 (2018) 468–478.
[29] B.D. Chung, S.W. Bae, S.W. Lee, C. Yoon, M.K. Hwang, K.D. Kim, J.J. Jeong, MARS Code Manual Volume V: Models and Correlations, Korea Atomic Energy Research Institute, 2010.
[30] J.M. Yoo, J.H. Kang, B.J. Yun, S.W. Hong, J.J. Jeong, Improvement of the MELCOR condensation heat transfer model for the thermal-hydraulic analysis of a PWR containment, Prog. Nucl. Energy 104 (2018) 172–182.
[31] E. Rahnm, Gothic Thermal Hydraulic Analysis Package Technical Manual Version 8.0 (QA), NAI 8907e06, Rev 19 (2012).
[32] T. Wang, D. Wang, L. Tong, X. Cao, Improvement of condensation model with the presence of non-condensable gas for thermal-hydraulic analysis in containment, Front. Energy Res. 9 (2021) 233.
[33] C. Popiel, J. Wojtkowiak, K. Bober, Laminar free convective heat transfer from isothermal vertical slender cylinder, Exp. Therm. Fluid Sci. 32 (2) (2007) 607–613.
[34] A. Dehbi, Correcting for tube curvature effects on condensation in the presence of a noncondensable gas in laminar regimes, Int. J. Heat Mass Tran. 151 (2020), 119384.
[35] J.-H. Hwang, D.-W. Jerng, An improved heat transfer model for steam-air mixture condensation with the curvature effect on vertical tubes, Int. Commun. Heat Mass Tran. 123 (2021), 105218.
[36] C. Wilke, C. Lee, Estimation of diffusion coefficients for gases and vapors, Ind. Eng. Chem. 47 (6) (1955) 1253–1257.
[37] B.E. Poling, J.M. Prausnitz, J.P. O'connell, The Properties of Gases and Liquids, Mcgraw-hill, New York, 2001.
[38] CD-adapco Inc, STAR-CCM+ 10.06 User Guide, 2015.
[39] J.O. Hirschfelder, C.F. Curtiss, R.B. Bird, M.G. Mayer, Molecular Theory of Gases and Liquids, Wiley, New York, 1954.
[40] C.L.V. Jayatilleke, The influence of Prandtl number and surface roughness on the resistance of the laminar sub-layer to momentum and heat transfer, Prog. Heat Mass Transfer 1 (1969).
[41] J.H. Sohn, H.Y. Yoon, Assessment of wall condensation models using CUPID code, in: Transactions of the Korean Nuclear Society Spring Meeting, 2018. Jeju, Korea.
[42] A. Dehbi, On the adequacy of wall functions to predict condensation rates from steam-noncondensable gas mixtures, Nucl. Eng. Des. 265 (2013) 25–34.
[43] F.P. Incropera, D.P. DeWitt, T.L. Bergman, A.S. Lavine, Fundamentals of Heat and Mass Transfer, Wiley, New York, 1996.
[44] T. Cebeci, Laminar-free-convective-heat transfer from the outer surface of a vertical slender circular cylinder, in: Heat Transfer 1974; Proceedings of the Fifth International Conference, vol. 3, 1974, pp. 15–19. Tokyo.
[45] J. Lee, G.-C. Park, H.K. Cho, Validation of Wall Film Condensation model in heat structure coupled CUPID-MARS, in: Transactions of the Korean Nuclear Society Autumn Meeting, Gyoung-Ju, Korea, 2017.
[46] H. Reynolds, T. Swearingen, D. McEligot, Thermal entry for low Reynolds number turbulent flow, J. Basic Eng. 91 (1969).